J. Appl. Comput. Mech., 11(3) (2025) 787-796
DOI: 10.22055/jacm.2024.47890.4818

ISSN: 2383-4536
jacm.scu.ac.ir

Shahid Chamran
University of Ahvaz

Journal of
Applied and Computational Mechanics

Research Paper

Mathematical Model of a Thermoelastic Micro-elongated Plate Influenced by Initial Stress and an Upper Load from a Piezoelectric Layer according to Dual-phase-lag Model

Mohamed I.A. Othman[1], Ebtesam E.M. Eraki[1], Mohamed F. Ismail[2]

[1] Department of Mathematics, Faculty of Science, Zagazig University, Zagazig 44519, Egypt
Email: m_i_a_othman@yahoo.com (M.I.A.O.); ebtesam.eraki@yahoo.com (E.E.M.E.)

[2] Faculty of Computers and Information System, Egyptian Chinese University, Cairo, Egypt
Email: m.fekry2015@yahoo.com

Received September 03 2024; Revised October 18 2024; Accepted for publication November 06 2024.
Corresponding author: M.I.A. Othman (m_i_a_othman@yahoo.com)

Abstract. The main goal of this work is to investigate how the initial stress affects a thermoelastic micro-elongated layer under a layer of piezoelectric loading using the theory of Lord-Shulman (L-S) with relaxation time and the model of dual-phase-lag (DPL) with two relaxation times. The normal mode analysis is used to transform the partial differential equations into ordinary differential equations. The numerical computations are carried out and the outcomes are visually presented. It is shown that initial stress has a significant impact on all physical quantities, as demonstrated by a comparison of the DPL model and the L-S theory in both full absence and presence of initial stress.

Keywords: Thermoelastic micro-elongated layer; piezoelectric; normal mode method; initial stress; DPL model.

1. Introduction

Four degrees of freedom model are presented in an elastic micro-elongated solid: one for micro-elongation and three for translation. The most recent micro-elongated theory states that only volumetric micro-elongated can be carried out in addition to the previous material particle average strain. Solid-liquid crystals, gas-filled porous media, and structural materials reinforced with chopped elastic fibers are other examples of micro-elongated media. A generalized theory of thermoelasticity has been extended to include deformations caused by internal heat sources in thermoelastic micro-elongated materials with h-thick elastic top layer [1]. Subsequently, recent studies [2] applied the earlier findings in a novel manner, changing the elastic layer's boundary from bounded to unbounded.

Shaw et al. [3] presented the effects of moving heat sources in homogeneous, isotropic, infinitely long, micro-elongated, thermoelastic materials. In addition to a user interface for liquid half-spaces and micro-elongated thermoelastic half-spaces, Sachdeva et al. [4] conducted research on the 2D deformation of these parts when mechanical forces are applied. Recent advances in single crystal growth techniques have been used to create piezo-ceramics with high voltage and substantial electrical breakdown [5]. According to Haussühl et al. [6], bismuth triborate (BiB_3O_6) is a nonlinear optical material with well-established piezo-electric and elastic properties.

By absorbing mechanical energy from the surrounding environment, nano fiber-based piezoelectric turbines can optimize energy for use in a range of electrical devices and hardware, according to Chang et al. [7]. A comprehensive study on virus-based piezoelectric power generation was conducted by Lee et al. [8]. Recently, results on nonlocal effects and temperature-dependent properties of the generic linear piezoelectric thermoelastic issue were presented in the literature [9].

It has been explored how to depict the general problem of steady-state vibrations of infinite piezoelectric medium [10]. Using different hypotheses, Othman et al. [11, 12] investigated how gravity affected the behavior of piezoelectric thermoelastic spinning medium. Tzou [13, 14] developed the DPL model, a novel heat transfer mechanism that approximates a version of Fourier's law by replacing Fourier's law with two distinct times. Tzou also provided two separate mathematical hyperbolic models for DPL heat transfer [14].

Published online: November 28 2024

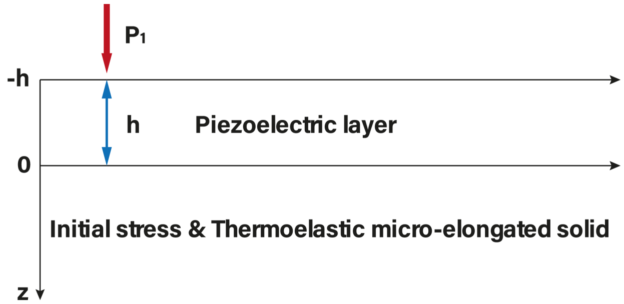

Fig. 1. Geometry of the problem.

Subsequently, Quintanilla et al. [15-17] examined the DPL thermoelastic system, they demonstrated how a half-group half-contraction gives rise to the problem's solution. The effect of initial stress on micro-elongated materials under on elastic layer was later examined using the DPL model [18], which is a DPL variant of the Fourier's law model. In the framework of fractional-order multiphase hysteresis models, a solution to the issue of thermoelastic interactions in functionally graded materials caused by thermal shock was investigated by Abbas [19]. In this regard, the following sources provide important details on the evolution of thermo-elastic theories in many fields [20-29].

Using the L-S theory and DPL model, as illustrated in Fig. 1, the main goal of this work is to investigate the effects of initial stress and the piezoelectric loading layer on thermoelastic micro-elongated media. Additionally, in the framework of DPL model, this work investigates the impact of relaxation time τ_θ period on all physical quantities.

2. Governing Equations

The same theories from [3, 21, 26] can be used to obtain the basic equations governing the behavior of micro-elongated thermoelasticity with initial stress using the DPL model as follows:

$$\sigma_{ij,j} = \rho u_{i,tt}, \tag{1}$$

$$a_0 \varphi_{,ii} + \beta_1 T - \lambda_1 \varphi - \lambda_0 u_{j,j} = \frac{1}{2} \rho j_0 \varphi_{,tt}, \tag{2}$$

$$k(1+\tau_\theta \frac{\partial}{\partial t})T_{,ii} = (1+\tau_q \frac{\partial}{\partial t})(\rho c_e \frac{\partial T}{\partial t} + \beta_0 T u_{k,kt}) + \beta_1 T_0 \varphi_{,t}, \tag{3}$$

$$\sigma_{ij} = 2\mu \varepsilon_{ij} + (\lambda e - \beta_0 T + \lambda_0 \varphi)\delta_{ij} - P(\delta_{ij} - w_{ij}). \tag{4}$$

where, $w_{ij} = (u_{j,i} - u_{i,j})/2$. For the vector of displacement $\mathbf{u}(x,z,t) = u(u_1, 0, u_3)$ and initial stress P, then, from Eqs. (1) and (4) we have:

$$\mu \nabla^2 u_1 + (\lambda+\mu) e_{,x} - \frac{P}{2}(u_{1,zz} - u_{3,xz}) - \beta_0 T_{,x} + \lambda_0 \varphi_{,x} = \rho u_{1,tt}, \tag{5}$$

$$\mu \nabla^2 u_3 + (\lambda+\mu) e_{,z} - \frac{P}{2}(u_{3,xx} - u_{1,xz}) - \beta_0 T_{,z} + \lambda_0 \varphi_{,z} = \rho u_{3,tt}. \tag{6}$$

For convenience, the dimensionless variables listed below can be used [30]:

$$\begin{gathered} x_i' = \frac{\omega^*}{c_1} x_i,\ z' = \frac{\omega^*}{c_1} z,\ u_i' = \frac{w^* c_1}{c_e T_0} u_i,\ t' = \omega^* t,\ \tau_\theta' = \omega^* \tau_\theta,\ \tau_q' = \omega^* \tau_q,\ \sigma_{ij}' = \frac{\sigma_{ij}}{\rho c_e T_0}, \\ \varphi' = \frac{\lambda_0}{\rho c_e T_0} \varphi,\ T' = \frac{T}{T_0},\ P' = \frac{P}{\lambda + 2\mu},\ P_1' = \frac{P_1}{\rho c_e T_0},\ w^* = \frac{\rho c_1^2 c_e}{k},\ c_1^2 = \frac{\lambda + 2\mu}{\rho}. \end{gathered} \tag{7}$$

By substituting in Eqs. (2), (3), (5), and (6) from dimensionless variables defined in Eq. (7), one obtains:

$$a_1 \nabla^2 u_1 + a_2 e_{,x} + \frac{P}{2}(u_{1,zz} - u_{3,xz}) - T_{,x} + \varphi_{,x} = u_{1,tt}, \tag{8}$$

$$a_1 \nabla^2 u_3 + a_2 e_{,z} + \frac{P}{2}(u_{3,xx} - u_{1,xz}) - T_{,z} + \varphi_{,z} = u_{3,tt}, \tag{9}$$

$$(\nabla^2 - a_4)\varphi + a_3 T - a_5 e = a_6 \varphi_{,tt}, \tag{10}$$

$$(1+\tau_\theta \frac{\partial}{\partial t})\nabla^2 T = (1+\tau_q \frac{\partial}{\partial t})[a_7 T_{,t} + a_8 e_{,t}] + a_9 \varphi_{,t}. \tag{11}$$

3. Method of Normal Mode

When operating in normal mode, the response for the recognized physical variables can be subjected to the following analysis:

$$[u_i, \varphi, T, \sigma_{ij}, u_i^p, \sigma_{ij}^p, D_i](x,z,t) = [u_i^*, \varphi^*, T^*, \sigma_{ij}^*, u_i^{p^*}, \sigma_{ij}^{p^*}, D_i^*](z) e^{(\omega t + ibx)}. \tag{12}$$

Using Eq. (12) into Eqs. (8)-(11), then one has:

$$[\delta_1 D^2 - \delta_2] u_1^* + \delta_3 D u_3^* - ibT^* + ib\varphi^* = 0, \tag{13}$$

$$\delta_3 D u_1^* + [\delta_4 D^2 - \delta_5] u_3^* - DT^* + D\varphi^* = 0, \tag{14}$$

$$-\delta_6 u_1^* - a_5 D u_3^* + a_3 T^* + [D^2 - \delta_7]\varphi^* = 0, \tag{15}$$

$$\delta_{10} u_1^* + \delta_{11} D u_3^* + [-\delta_8 D^2 + \delta_{12}] T^* + \delta_{13} \varphi^* = 0. \tag{16}$$

There is a non-trivial solution to Eqs. (13) through (16). If the determinant of the coefficient of the physical quantity equals to zero:

$$(D^8 - AD^6 + BD^4 - CD^2 + E)\{u_1^*(z), u_3^*(z), T^*(z), \varphi^*(z)\} = 0. \tag{17}$$

Equation (18) can be factorized as:

$$(D^2 - k_1^2)(D^2 - k_2^2)(D^2 - k_3^2)(D^2 - k_4^2)\{u_1^*(z), u_3^*(z), T^*(z), \varphi^*(z)\} = 0, \tag{18}$$

where $k_n^2, (n = 1,2,3,4)$ indicates the roots of the auxiliary Eq. (18). Since $z \to \infty$, the generalized solution of Eq. (18) is given by:

$$(u_1^*, u_3^*, T^*, \varphi^*)(z) = \sum_{n=1}^{4} (1, H_{1n}, H_{2n}, H_{3n}) M_n e^{-k_n z}. \tag{19}$$

The components of stresses can be entered into (4) by substituting from Eqs. (7), (19):

$$(\sigma_{xx}, \sigma_{zz})(z) = \sum_{n=1}^{4} (H_{4n}, H_{5n}) M_n e^{(-k_n z + \omega t + ibx)} - a_{11} P, \tag{20}$$

$$\sigma_{xz}(z) = \sum_{n=1}^{4} H_{6n} M_n e^{(-k_n z + \omega t + ibx)}. \tag{21}$$

where the coefficients $a_1, a_2, \ldots, a_{13}$, $\delta_1, \delta_2, \ldots, \delta_{13}$, A, B, C, E, $H_{1n}, H_{2n}, H_{3n}, H_{4n}, H_{5n}$ and H_{6n} are obtained from Appendix 1.

The governing equations of general piezoelectric are [31]:

$$\sigma_{ij,j}^p = \rho^p u_{i,tt}^p, \tag{22}$$

$$D_{i,i} = 0, \tag{23}$$

$$\sigma_{ij}^p = \frac{1}{2} C_{ijkl}(u_{k,l}^p + u_{l,k}^p) - e_{kij} E_k, \tag{24}$$

$$D_i = \frac{1}{2} e_{ijk}(u_{j,k}^p + u_{k,j}^p) + \in_{ij} E_j. \qquad E_i = -\varphi_{,i}^p. \tag{25}$$

The non-dimensional variables mentioned below can be used to simplify parameters and equations:

$$x^{p'} = c_0 \eta_0 x^p,\ z^{p'} = c_0 \eta_0 z^p,\ u_i^{p'} = c_0 \eta_0 u_i^p,\ t^{p'} = c_0^2 \eta_0 t^p,\ \sigma_{ij}^{p'} = \frac{\sigma_{ij}^p}{C_{11}},\ D_i' = \frac{D_i}{e_{33}},\ c_0^2 = \frac{c_{11}}{\rho^p},\ \varphi^{p'} = \frac{\in_{11} c_0 \eta_0}{e_{33}} \varphi^p,\ \eta_0 = \frac{\rho^p c_e^p}{k^p}. \tag{26}$$

Utilizing Eqs. (26) and (12) into Eqs. (22) and (23):

$$(l_1 D^2 - A_1)u_1^{p*} + ibl_2 Du_3^{p*} + ibl_3 D\varphi^{p*} = 0, \tag{27}$$

$$ibl_2 Du_1^{p^*} + (l_5 D^2 - A_2)u_3^{p*} + (l_7 D^2 - b^2 l_6)\varphi^{p*} = 0, \tag{28}$$

$$ibl_8 Du_1^{p*} + (D^2 - b^2 l_9)u_3^{p*} + (-l_{10} D^2 + b^2)\varphi^{p*} = 0. \tag{29}$$

Eliminating $u_1^{p^*}$, $u_3^{p^*}$, φ^{p*} between Eqs. (27) to (29), then:

$$(D^6 - GD^4 + ND^2 - F)\{u_1^{p*}(z),\ u_1^{p*}(z),\ \varphi^{p*}(z)\} = 0. \tag{30}$$

Equation (32) can be factorized as:

$$(D^2 - r_1^2)(D^2 - r_2^2)(D^2 - r_3^2)\{u_1^{p*}(z),\ u_1^{p*}(z),\ \varphi^{p*}(z)\} = 0. \tag{31}$$

When the roots of auxiliary equation of Eq. (31) are $r_i^2, (i=1,2,3)$, and the following are the solutions to Eq. (31):

$$(u_1^{p*}, u_3^{p*}, \varphi^{p*})(z) = \sum_{i=1}^{3}(1, L_{1i}, L_{2i})R_i e^{-r_i z} + \sum_{i=1}^{3}(1, L_{1(i+3)}, L_{2(i+3)})R_{i+3} e^{r_i z}. \tag{32}$$

Using Eqs. (26), (12) and (32) in Eq. (24) and (25) to derive the electric displacement and stress components in the piezoelectric layer, one obtains:

$$(\sigma_{xx}^{p*}, \sigma_{zz}^{p*}, \sigma_{xz}^{p*})(z) = \sum_{i=1}^{3}(L_{3i}, L_{4i}, L_{5i})R_i e^{-r_i z} + \sum_{i=1}^{3}(L_{3(i+3)}, L_{4(i+3)}, L_{5(i+3)})R_i e^{r_i z}, \tag{33}$$

$$(D_x^*, D_z^*)(z) = \sum_{i=1}^{3}(L_{6i}, L_{7i})R_i e^{-r_i z} + \sum_{i=1}^{3}(L_{6(i+3)}, L_{7(i+3)})R_{i+3} e^{r_i z}. \tag{34}$$

where, the coefficients $l_1, l_2, \ldots, l_{13}$, A_1, A_2, G, N, F, L_{mi} and $L_{mi}, (m=1,2,3,4,5,6)$ can be found in Appendix 2

4. The Situation at the Borders

It is necessary to choose the parameters $M_1, M_2, M_3, M_4, R_1, R_2, R_3, R_4, R_5, R_6$, so that the surface boundary conditions are:

$$\sigma_{zz} = \sigma_{zz}^{p} - a_{11} P,\ \sigma_{xz} = \sigma_{xz}^{p},\ u_1 = u_1^{p},\ u_3 = u_3^{p},\ \varphi = 0,\ \frac{\partial T}{\partial z} = 0,\ D_x = 0,\ D_z = 0 \ \text{at}\ z = 0. \tag{35}$$

$$\sigma_{zz} = \sigma_{zz}^{p} - P_1 e^{(\omega t + ibx)} - a_{11} P,\ \sigma_{xz} = 0,\ \text{at}\ z = -h. \tag{36}$$

The characteristic equations can be easily obtained from the previous boundary conditions. Ten equations are subjected to the inverse method matrix in order to obtain the parameters $M_n, (n = 1,2,3,4)$ and $R_{n'}, (n' = 1,2,3,4,5,6)$:

$$\begin{bmatrix} M_1 \\ M_2 \\ M_3 \\ M_4 \\ R_1 \\ R_2 \\ R_3 \\ R_4 \\ R_5 \\ R_6 \end{bmatrix} = \begin{bmatrix} H_{51} & H_{52} & H_{53} & H_{54} & -L_{41} & -L_{42} & -L_{43} & -L_{44} & -L_{45} & -L_{46} \\ H_{61} & H_{62} & H_{63} & H_{64} & -L_{51} & -L_{52} & -L_{53} & -L_{54} & -L_{55} & -L_{56} \\ 1 & 1 & 1 & 1 & -1 & -1 & -1 & -1 & -1 & -1 \\ H_{11} & H_{12} & H_{13} & H_{14} & -L_{11} & -L_{12} & -L_{13} & -L_{14} & -L_{15} & -L_{16} \\ H_{31} & H_{32} & H_{33} & H_{34} & 0 & 0 & 0 & 0 & 0 & 0 \\ -k_1 H_{21} & -k_2 H_{22} & -k_3 H_{23} & -k_4 H_{24} & 0 & 0 & 0 & 0 & 0 & 0 \\ 0 & 0 & 0 & 0 & L_{61} & L_{62} & L_{63} & L_{64} & L_{65} & L_{66} \\ 0 & 0 & 0 & 0 & L_{71} & L_{72} & L_{73} & L_{74} & L_{75} & L_{76} \\ H_{51}e^{k_1 h} & H_{52}e^{k_2 h} & H_{53}e^{k_3 h} & H_{54}e^{k_4 h} & -L_{41}e^{r_1 h} & -L_{42}e^{r_2 h} & -L_{43}e^{r_3 h} & -L_{44}e^{-r_1 h} & -L_{45}e^{-r_2 h} & -L_{46}e^{-r_3 h} \\ H_{61}e^{k_1 h} & H_{62}e^{k_2 h} & H_{63}e^{k_3 h} & H_{64}e^{k_4 h} & 0 & 0 & 0 & 0 & 0 & 0 \end{bmatrix}^{-1} \begin{bmatrix} 0 \\ 0 \\ 0 \\ 0 \\ 0 \\ 0 \\ 0 \\ 0 \\ -P_1 \\ 0 \end{bmatrix}. \tag{37}$$

5. The Numerical Results and Discussion

Aluminum epoxy-like material has been used for conducting the analysis (see Table 1) [32]. Cadmium Selenide (CdSe), with hexagonal symmetry (6 mm class), is the material selected for the piezoelectric device (see Table 2) [30]. In this work, calculations are carried out in the range $0 \le z \le 3$ at $x = 0.005$ for time $t = 1.02$. To examine how the initial stress affects the DPL model, the L-S theory, and the temperature gradient Tc's phase shift affect the DPL model of constant phase lag on heat flow τ_q, the components of displacement u_1, u_3, the micro-elongated scalar φ, and the component of stress σ_{xz} were distributed with a distance of z, using the numerical analysis method. Graphs representing the outcomes of numerical estimation are presented in this work.

Table 1. The material properties of Aluminum epoxy.

$\lambda = 7.59\times10^{10}\ \mathrm{N/m^2}$	$\mu = 1.89\times10^{10}\ \mathrm{N/m^2}$	$\rho = 2.19\times10^{3}\ \mathrm{kg/m^3}$
$a_0 = 0.61\times10^{-10}\ \mathrm{N}$	$c_e = 966\ \mathrm{J/kg.k}$	$j_0 = 0.196\times10^{-4}\ \mathrm{m^2}$
$\beta_0 = \beta_1 = 0{,}05\times10^{5}\ \mathrm{N/m^2.k}$	$k = 252\ \mathrm{J/m.s.k}$	$\lambda_0 = \lambda_1 = 0.37\times10^{10}\ \mathrm{N/m^2}$
$T_0 = 293\ \mathrm{K}$	$\tau_\theta = 1\times10^{-4}\ \mathrm{s}$	$\tau_q = 9\times10^{-3}\ \mathrm{s}$
$\omega = \omega_0 + i\zeta$	$\omega_0 = -2\times10^{-4},\ \zeta = -3.6\times10^{-3}$	$b = 3,\ h = 0.02$

Table 2. The material properties of Cadmium Selenide.

$C_{11} = 7.41\times10^{10}\ \mathrm{N.m^{-2}}$	$C_{13} = 3.93\times10^{10}\ \mathrm{N.m^{-2}}$	$C_{33} = 8.36\times10^{10}\ \mathrm{N.m^{-2}}$
$C_{44} = 1.32\times10^{10}\ \mathrm{N.m^{-2}}$	$\rho = 5504\ \mathrm{kg.m^{-3}}$	$e_{31} = -0.160\ \mathrm{C.m^{-2}}$
$e_{33} = 0.347\ \mathrm{C.m^{-2}}$	$e_{15} = -0.138\ \mathrm{C.m^{-2}}$	$c_e^p = 260\ \mathrm{J/kg.k}$
$\in_{11} = 8.26\times10^{-11}\ \mathrm{C^2.N^{-1}.m^{-2}}$	$\in_{33} = 9.03\times10^{-11}\ \mathrm{C^2.N^{-1}.m^{-2}}$	

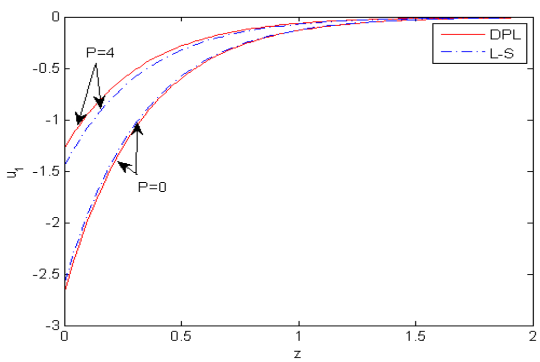

Fig. 2. Influence of initial stress on the horizontal displacement u_1.

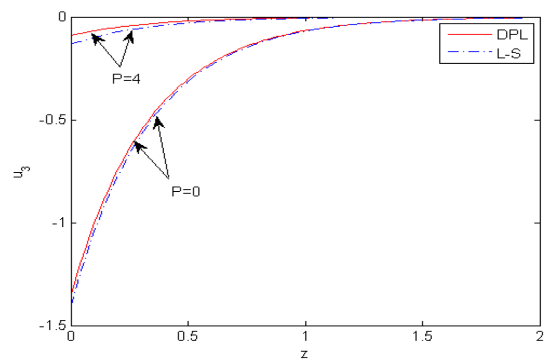

Fig. 3. Influence of initial stress on the vertical displacement u_3.

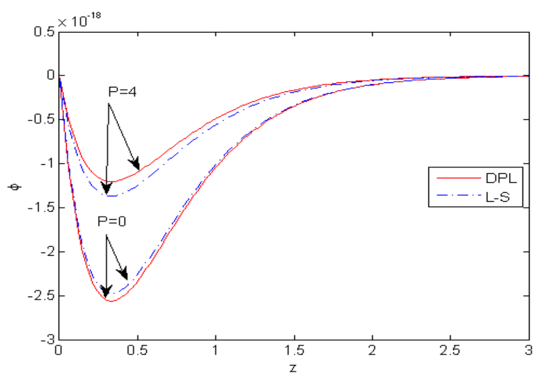

Fig. 4. Influence of initial stress on the micro-elongated scalar φ.

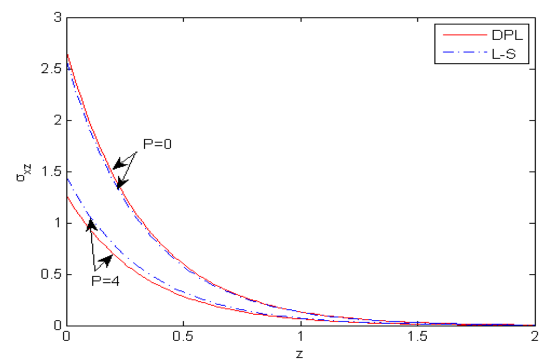

Fig. 5. Influence of initial stress on the force stress component σ_{xz}.

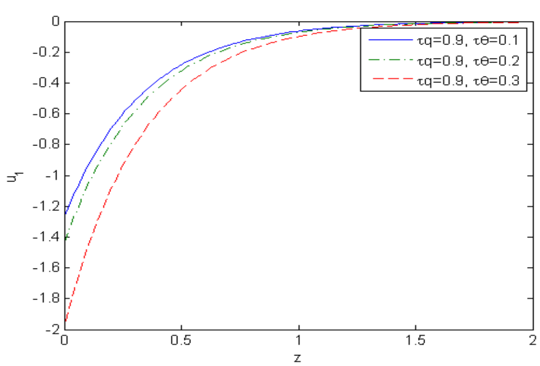

Fig. 6. Influence of τ_θ on the horizontal displacement u_1 at $P = 4$.

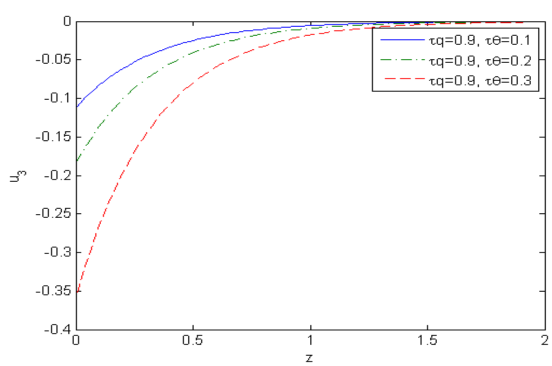

Fig. 7. Influence of τ_θ on the vertical displacement u_3 at $P = 4$.

The outcomes of the two earlier theories for a mechanical force of magnitude $P_1 = 0.3$ are displayed in Figs. 2 to 9. Figures 2 to 5 compare physical quantities with and without an initial stress.

The distribution of u_1 with Z is displayed in Fig. 2. In the theory of (L-S) and (DPL) model, it is clear that the values of u_1 are less without initial stress than they are with initial stress. The values of u_1 grow until they reach zero. Figure 3 clarifies that based on the (L-S) theory and the (DPL) model, the values of u_3 increase with increase z for $(P=0,4)$. In the case of $P=4$, it is clear that the values of u_3 go to zero with increasing of z at $z \geq 1$, as well as in the case $P=0$ the values of u_3 go to zero with increasing of z at $z \geq 1.6$. Figure 4 explains that the distribution of the micro-elongated φ starts from zero in the two theories for (P= 0, 4). Evidently, over the range $0 \leq z \leq 0.4$, the four curves of φ begin to decline to a minimum value, and over the range $0.4 \leq z \leq 2.5$ they decrease all the way to zero. Figure 5 illustrates that in both the model of (DPL) and theory of (L-S), σ_{xz} always begins at a positive value for $(P=0,4)$. The values of σ_{xz} are found to vanish at $z > 1.7$. Furthermore, it is clear that the values of σ_{xz} based on $P=4$ are lower than the ones based on $P=0$. The distribution of u_1, u_3, σ_{xz} with z and the microelongational scalar φ under the impact of initial stress on the model of (DPL) for the various phase-lag of temperature gradient τ_θ values are plotted in Figs. 6 to 9. The following values are found at $\tau_q = 0.9,\ \tau_\theta = 0.1,\ 0.2,\ 0.3$.

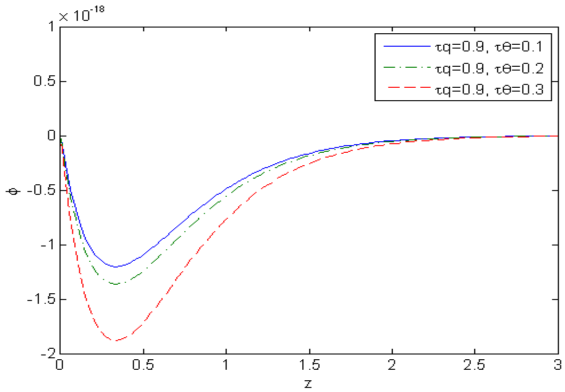

Fig. 8. Influence of τ_θ on the micro-elongated scalar φ at P = 4.

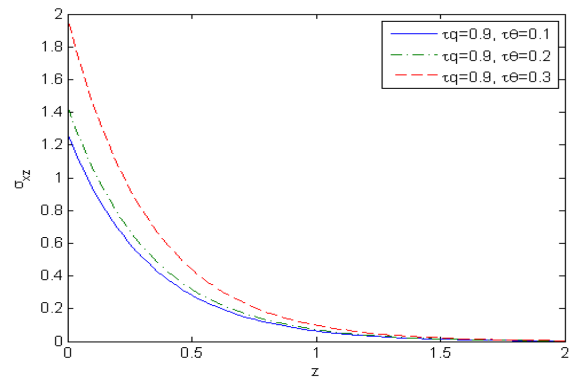

Fig. 9. Influence of τ_θ on the force stress component σ_{xz} at P = 4.

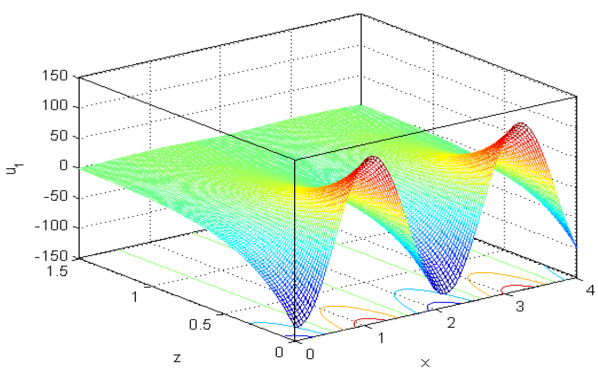

Fig. 10. Three-dimension curve variation of the horizontal displacement u_1 versus distances at $P=4, \tau_\theta = 1\times 10^{-4}, \tau_q = 9\times 10^{-3}$.

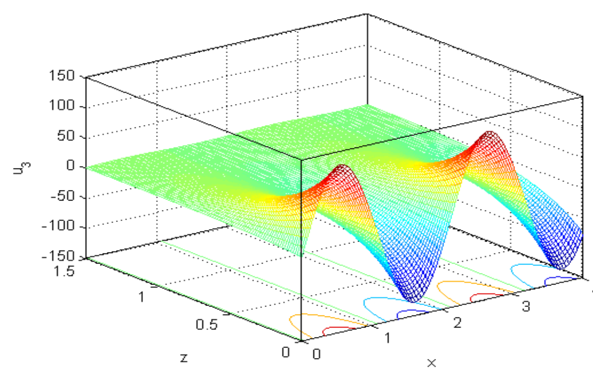

Fig. 11. Three-dimension curve variation of the vertical displacement u_3 versus distances at $P=4, \tau_\theta = 1\times 10^{-4}, \tau_q = 9\times 10^{-3}$.

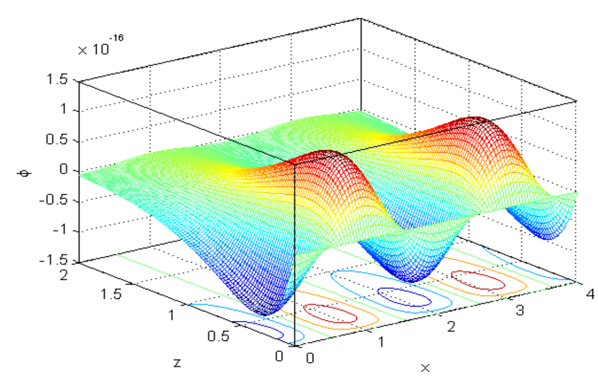

Fig. 12. Three-dimension curve variation of the micro-elongated scalar φ versus distances at $P=4, \tau_\theta = 1\times 10^{-4}, \tau_q = 9\times 10^{-3}$.

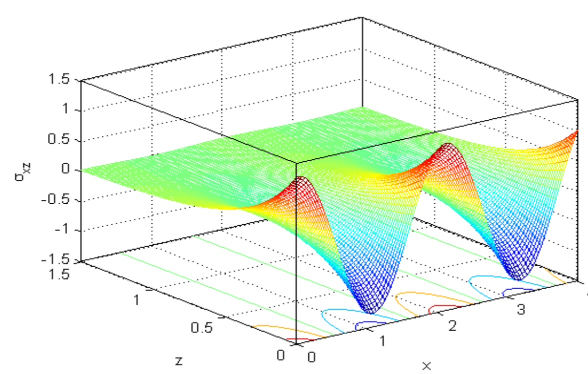

Fig. 13. Three-dimension curve variation of the stress component σ_{xz} versus distances at $P=4, \tau_\theta = 1\times 10^{-4}, \tau_q = 9\times 10^{-3}$.

Figures 6 and 7 exhibit that the effect of τ_θ on u_1 and u_3 are decreasing over the range $0 \le z \le 1.7$. Figure 8 describes the distribution of micro-elongated φ versus z. The three curves clearly begin at zero, fall to a minimum value over the range $0 \le z \le 0.4$, and decrease back to zero over $0.4 \le z \le 2.5$. Furthermore, it is evident that the impact of τ_θ on micro-elongated φ is waning. The distribution of σ_{xz} vs z is displayed in Fig. 9.

The three-dimensional (3D) plotting of Figs. 10 to 13, show the relationship between the physical quantities u_1, u_3, φ and σ_{xz} with both (x,z) at $P=4$ under the model of (DPL). These numbers are essential for understanding the connections between these real numbers and the vertical component of distance. All of the field quantities are moving in wave propagations, and the resultant curves are heavily dependent on the vertical distance.

6. Conclusion

The mathematical model presented for a thermoelastic micro-elongated plate influenced by initial stress and subjected to an upper load from a piezoelectric layer, within the framework of the (DPL) model, offers a detailed insight into the coupled behavior of thermal, elastic, and electric fields. By incorporating the effects of initial stress and piezoelectric interaction, this model broadens the understanding of complex physical phenomena in micro-elongated materials. The use of the (DPL) model allows for a more accurate representation of thermal and mechanical wave propagation by accounting for phase lags in both heat flux and temperature gradients. The main conclusions are as follows:

- A comparison was made between the (DPL) model and (L-S) theory, both with and without the presence of initial stress.
- In the context of thermoelastic medium deformation, the initial stress and micro-elongation scalar play pivotal roles.
- The amplitude of the field quantities shows a decreasing trend with increasing relaxation time, highlighting the significant influence of the relaxation time parameter.
- A decomposition solution is provided for the thermoelastic micro-elongated layer, covered by a finite elastic layer, under the effect of initial stress.

The results obtained in this study emphasize the sensitivity of the plate's behavior to the initial stress, material properties, and external loads, making this model a valuable tool in the design and analysis of micro-scale thermoelastic systems. Future extensions of this work may include nonlinearities, more complex boundary conditions, or dynamic load applications, providing a more comprehensive understanding of such systems under varying physical conditions.

Author Contributions

M.I.A. Othman planned the scheme, initiated the project, and examined the theory validation. E.E.M. Eraki and M.F. Ismail developed the mathematical modeling and analyzed the results. The manuscript was written through the contribution of all authors. All authors discussed the results, reviewed, and approved the final version of the manuscript.

Acknowledgment

Not applicable.

Conflicts of interest

The authors declared no potential conflicts of interest concerning the research, authorship, and publication of this article.

Funding

There is no funding available for this research article.

Data Availability Statements

The datasets generated and/or analyzed during the current study are available from the corresponding author on reasonable request.

Nomenclature

λ, μ	Lame's constants in micro-elongated medium	P	Initial pressure
ε_{ij}	The strain tensor where $\varepsilon_{ij} = (u_{i,j} + u_{j,i})/2$	c_e	Specific heat at the constant strain in micro-elongated medium
ρ	Density in micro-elongated medium	ρ^p	Density in piezoelectric layer
$\mathbf{u}$	Displacement vector in micro-elongated medium	φ	Micro-elongational scalar
c_e^p	Specific heat at constant strain in piezoelectric layer	σ_{ij}	Component of stress tensor for micro-elongated medium
$\mathbf{u}^p$	Displacement vector in piezoelectric layer	E_i	Electric field in piezoelectric layer
C_{ijkl}	The elastic parameters tensor in piezoelectric	T	Absolute temperature
k^p	Thermal conductivity in piezoelectric layer	T_0	Reference temperature
D_i	The electric displacement in piezoelectric layer	j_0	Microinertia
$\in_{ij}$	The dielectric moduli in piezoelectric layer	ω	A complex constant
e_{kij}	The piezo electric moduli in piezoelectric layer	τ_θ	Temperature gradient parameter

φ^p	The electric potential in piezoelectric layer	τ_q	Heat flux parameter
P_1	The magnitude of the mechanical force.	i	$=\sqrt{-1}$
k	Thermal conductivity in micro-elongated medium	$a_0, \lambda_0, \lambda_1$	Micro-elongational constants
α_{t1}, α_{t2}	The coefficients of linear thermal expansion where $\beta_0 = (3\lambda + 2\mu)\alpha_{t1}$, $\beta_1 = (3\lambda + 2\mu)\alpha_{t2}$	b	The wave number in the x direction.

References

[1] Ailawalia, P., Sachdeva, S.K., Pathania, D.S., Plane strain deformation in a thermo-elastic microelongated solid with internal heat source, *International Journal of Applied Mechanics and Engineering*, 20(4), 2015, 717-731.
[2] Ailawalia, P., Sachdeva, S.K., Pathania, D.S., Internal heat source in thermo-elastic micro-elongated solid under Green-Lindsay theory, *Journal of Theoretical and Applied Mechanics*, 46(2), 2016, 65-82.
[3] Shaw, S., Mukhopadhyay, B., Moving heat source response in a thermoelastic microelongated solid, *Journal of Engineering Physics and Thermophysics*, 86(3), 2013, 716–722.
[4] Sachdeva, S.K., Ailawalia, P., Plane strain deformation in thermoelastic micro-elongated solid, *Civil and Environmental Research*, 7(2), 2015, 92-98.
[5] Tichý, J., Erhart, J., Kittinger, E., Privratska, J., Fundamentals of piezoelectric sensorics: mechanical, dielectric, and thermodynamical properties of piezoelectric materials, *Springer Science & Business Media*, 2010.
[6] Haussühl, S., Bohatý, L., Becker, P., Piezoelectric and elastic properties of the non-linear optical material bismuth triborate, BiB3O6, *Applied Physics A*, 82(3), 2006, 495-502.
[7] Chang, J., Dommer, M., Chang, C., Lin, L., Piezoelectric nanofibers for energy scavenging applications, *Nano Energy*, 1(3), 2012, 356-371.
[8] Lee, B.Y., Zhang, J., Zueger, C., Chung, W.J., Yoo, S.Y., Wang, E., Lee, S.W., Virus based piezo-electric energy generation, *Nature Nanotechnology*, 7(6), 2012, 351-356.
[9] Li, D., He, T., Investigation of generalized piezoelectric-thermoelastic problem with nonlocal effect and temperature-dependent properties, *Heliyon*, 4(10), 2018, e00860.
[10] Lioubimova, E., Schiavone, P., Steady-state vibrations of an unbounded linear piezoelectric medium, *Journal of Applied Mathematics and Physics*, 57, 2006, 862- 874.
[11] Othman, M.I.A., Ahmed, E.A.A., The effect of rotation on piezo-thermoelastic medium using different theories, *Structural Engineering and Mechanics*, 56(4), 2015, 649-665.
[12] Othman, M.I.A., Ahmed, E.A., Effect of gravity field on piezo-thermoelastic medium with three theories, *Journal of Thermal Stresses*, 39(4), 2016, 474-486.
[13] Tzou, D.Y., The generalized lagging response in small-scale and high-rate heating, *International Journal of Heat Mass Transfer*, 38(17), 1995, 3231–3240.
[14] Tzou, D.Y., A unified approach for heat conduction from macro to microscales, *Journal of Heat Transfer*, 117(1), 1995, 8–16.
[15] Quintanilla, R., Racke, R., A note on stability of dual-phase-lag heat conduction, *International Journal of Heat Mass Transfer*, 49(7-8), 2006, 1209–1213.
[16] Quintanilla, R., Racke, R., Qualitative aspects in dual-phase-lag thermoelasticity, *Siam Journal of Applied Mathematics*, 66(3), 2006, 977–1001.
[17] Quintanilla, R., Exponential stability in the dual-phase-lag heat conduction theory, *Journal of Non-Equilibrium Thermodynamics*, 27(3), 2002, 217–227.
[18] Othman, M.I.A., Atwa, S.Y., Eraki, E.E.M., Ismail, M.F., A thermoelastic micro- elongated layer under the effect of gravity in the context of the dual-phase-lag model, *Journal of Applied Mathematics and Mechanics*, 101(12), 2021, e202100109.
[19] Abbas, I.A., Generalized thermoelastic interaction in functional graded material with fractional order three-phase lag heat transfer, *Journal of Central South University*, 22(5), 2015, 1606-1613.
[20] Othman, M.I.A., Song, Y., Reflection of plane waves from an elastic solid half- space under hydrostatic initial stress without energy dissipation, *International Journal of Solids and Structures*, 44, 2007, 5651-5664.
[21] Othman, M.I.A., Abd-Elaziz, E.M., Effect of initial stress and hall current on a magneto-thermoelastic porous medium with micro-temperatures, *Indian Journal of Physics*, 93(4), 2019, 475-485.
[22] Abd-Elaziz, E.M., Marin, M., Othman, M.I.A., On the effect of Thomson and initial stress in a thermo-porous elastic solid under GN electromagnetic theory, *Symmetry*, 11(3), 2019, 413-430.
[23] Othman, M.I.A., Abouelregal, A.E., Said, S.M., The effect of variable thermal conductivity on an infinite fiber-reinforced thick plate under initial stress, *Journal of Mechanics of Materials and Structures*, 14(2), 2019, 277-293.
[24] Marin, M., Agarwal, R.P., Mahmoud, S.R., Nonsimple material problems addressed by the Lagrange's identity, *Boundary Value Problems*, 2013, 2013, 135.
[25] Marin, M., Agarwal, R.P., Mahmoud, S.R., Modeling a microstretch thermoelastic body with two temperatures, *Abstract and Applied Analysis*, 2013, 2013, 583464.
[26] Othman, M.I.A., Atwa, S.Y., Eraki, E.E.M., Ismail, M.F., The initial stress effect on a thermoelastic micro-elongated solid under the dual-phase-lag model, *Applied Physics A*, 127(9), 2021, 697-704.
[27] Vlase, S., Marin, M., Scutaru, M.L., Munteanu, R., Coupled transverse and torsional vibrations in a mechanical system with two identical bears, *AIP Advances*, 7(6), 2017, 065301.
[28] Marin, M., Öchsner, A., Bhatti, M.M., Some results in Moore-Gibson-Thompson thermoelasticity of dipolar bodies, *ZAMM-Journal of Applied Mathematics and Mechanics*, 100(12), 2020, e202000090.
[29] Vlase, S., et al., A method for the study of the vibration of mechanical bars systems with symmetries, *Acta Tech. Napocensis, Ser. Appl. Math. Mech. Eng.*, 60(4), 2017, 539–544.
[30] Ashmat, A., Adnan, J., Aftab, K., Reflection of thermoelastic wave in semi-conductor nano-structures nonlocal porous medium, *Journal of Central South University*, 27(11), 2020, 3188-3201.
[31] Ahmed, E.A., Abou-Dina, M.S., El Dhaba, A.R., Effect of gravity on piezo-thermo-elasticity within the dual-phase-lag model, *Microsystem Technologies*, 25(1), 2019, 1-10.
[32] Ailawalia, P., Sachdeva, S.K., Pathania, D.S., A two-dimensional problem on laser pulse heating in thermoelastic microelongated solid, *Archives of Thermodynamics*, 40(2), 2019, 69-85.

Appendix 1

$$a_1 = \frac{\mu}{\rho c_1^2},\ a_2 = \frac{\lambda+\mu}{\rho c_1^2},\ a_3 = \frac{\beta_1 \lambda_0 c_1^2}{a_0 \rho c_e \omega^{*2}},\ a_4 = \frac{\lambda_1 c_1^2}{a_0 \omega^{*2}},\ a_5 = \frac{\lambda_0^2}{a_0 \rho \omega^{*2}},\ a_6 = \frac{\rho j_0 c_1^2}{2a_0},\ a_7 = \frac{\rho c_e c_1^2}{k\omega^*}, \tag{1.1}$$

$$a_8 = \frac{\beta_0^2 T_0}{k\rho\omega^*},\ a_9 = \frac{\beta_0 \beta_1 T_0 c_1^2}{k\lambda_0 \omega^*},\ a_{10} = \frac{\lambda}{\rho c_1^2},\ a_{11} = \frac{\lambda+2\mu}{\rho c_e T_0},\ a_{12} = \frac{\mu+\frac{1}{2}(\lambda+2\mu)P}{\rho c_1^2},\ a_{13} = \frac{\mu-\frac{1}{2}(\lambda+2\mu)P}{\rho c_1^2}, \tag{1.2}$$

$$\delta_1 = a_1 + \frac{P}{2},\ \delta_2 = a_1 b^2 + a_2 b^2 + \omega^2,\ \delta_3 = ib(a_2 - \frac{P}{2}),\ \delta_4 = a_1 + a_2,\ \delta_5 = a_1 b^2 + \frac{P}{2} b^2 + \omega^2,\ \delta_6 = iba_5,\ \delta_7 = b^2 + a_4 + a_6\omega^2, \tag{1.3}$$

$$\delta_8 = 1 + \tau_\theta \omega,\ \delta_9 = 1 + \tau_q \omega,\ \delta_{10} = iba_8 \omega \delta_9,\ \delta_{11} = a_8 \omega \delta_9,\ \delta_{12} = b^2 \delta_8 + a_7 \omega \delta_9,\ \delta_{13} = a_9 \omega, \tag{1.4}$$

$$A = \frac{-1}{\delta_1 \delta_4 \delta_8}[a_5 \delta_1 \delta_8 - \delta_1 \delta_5 \delta_8 - \delta_2 \delta_4 \delta_8 - \delta_3^2 \delta_8 - \delta_1 \delta_4 \delta_{12} - \delta_1 \delta_4 \delta_7 \delta_8], \tag{1.5}$$

$$\begin{aligned} B = \frac{1}{\delta_1 \delta_4 \delta_8}[&\delta_2 \delta_{11} + \delta_3 \delta_{10} - a_3 \delta_1 \delta_{11} - a_5 \delta_2 \delta_8 - a_5 \delta_1 \delta_{12} - a_5 \delta_1 \delta_{13} + ib\delta_3 \delta_{11} - ib\delta_4 \delta_{10} + \delta_2 \delta_5 \delta_8 - \delta_3 \delta_6 \delta_8 + \delta_1 \delta_5 \delta_{12} + \delta_2 \delta_4 \delta_{12} \\ &+ \delta_3^2 \delta_{12} + \delta_1 \delta_7 \delta_{11} - ia_5 b \delta_3 \delta_8 + a_3 \delta_1 \delta_4 \delta_{13} + ib\delta_4 \delta_6 \delta_8 + \delta_1 \delta_5 \delta_7 \delta_8 + \delta_2 \delta_4 \delta_7 \delta_8 + \delta_3^2 \delta_7 \delta_8 + \delta_1 \delta_4 \delta_7 \delta_{12}], \end{aligned} \tag{1.6}$$

$$\begin{aligned} C = \frac{-1}{\delta_1 \delta_4 \delta_8}[&a_3 \delta_2 \delta_{11} + a_3 \delta_3 \delta_{10} + a_5 \delta_2 \delta_{12} + a_5 \delta_2 \delta_{13} + ib\delta_5 \delta_{10} - \delta_2 \delta_5 \delta_{12} - \delta_2 \delta_7 \delta_{11} - \delta_3 \delta_7 \delta_{10} + \delta_3 \delta_6 \delta_{12} + \delta_3 \delta_6 \delta_{13} + iba_3 \delta_3 \delta_{11} - iba_3 \delta_4 \delta_{10} + iba_5 \delta_3 \delta_{12} \\ &+ iba_5 \delta_4 \delta_{13} - a_3 \delta_1 \delta_5 \delta_{13} - a_3 \delta_2 \delta_4 \delta_{13} - a_3 \delta_3^2 \delta_{13} - ib\delta_5 \delta_6 \delta_8 - ib\delta_3 \delta_7 \delta_{11} + ib\delta_4 \delta_7 \delta_{10} - ib\delta_4 \delta_6 \delta_{12} - ib\delta_4 \delta_6 \delta_{13} - \delta_2 \delta_5 \delta_7 \delta_8 - \delta_1 \delta_5 \delta_7 \delta_{12} - \delta_2 \delta_4 \delta_7 \delta_{12} - \delta_3^2 \delta_7 \delta_{12}], \end{aligned} \tag{1.7}$$

$$H_{1n} = \frac{k_n \delta_2 + ibk_n \delta_3 - \delta_1 k_n^3}{(ib\delta_4 - \delta_3)k_n^2 - ib\delta_5},\quad H_{2n} = \frac{k_n^3 \delta_{11} H_{1n} + a_5 \delta_{11} k_n H_{1n} + \delta_7 \delta_{11} H_{1n} k_n - k_n^2 \delta_{10} - \delta_6 \delta_{13} + \delta_7 \delta_{10}}{\delta_7 \delta_8 k_n^2 + \delta_{12} k_n^2 - \delta_8 k_n^4 - \delta_7 \delta_{12} - a_3 \delta_{13}}, \tag{1.8}$$

$$H_{3n} = \frac{a_5 k_n H_{1n} + a_3 H_{2n} - \delta_6}{\delta_7 - k_n^2},\ H_{4n} = ib - a_{10} k_n H_{1n} - H_{2n} + H_{3n}, \tag{1.9}$$

$$H_{5n} = iba_{10} - k_n H_{1n} - H_{2n} + H_{3n},\ H_{6n} = iba_{13} H_{1n} - a_{12} k_n. \tag{1.10}$$

Appendix 2

$$l_1 = \frac{C_{44}}{C_{11}},\ l_2 = \frac{C_{44} + C_{13}}{C_{11}},\ l_3 = \frac{(e_{31} + e_{15})e_{33}}{\in_{11} C_{11}},\ l_4 = \frac{\rho^p c_0^2}{C_{11}},\ l_5 = \frac{C_{33}}{C_{11}},\ l_6 = \frac{e_{15} e_{33}}{\in_{11} C_{11}},\ l_7 = \frac{e_{33}^2}{\in_{11} C_{11}}, \tag{2.1}$$

$$l_8 = \frac{e_{31} + e_{15}}{e_{33}},\ l_9 = \frac{e_{15}}{e_{33}},\ l_{10} = \frac{\in_{33}}{\in_{11}},\ l_{11} = \frac{C_{13}}{C_{11}},\ l_{12} = \frac{e_{31} e_{33}}{\in_{11} C_{11}},\ l_{13} = \frac{e_{31}}{e_{33}},\ A_1 = b^2 + l_4 \omega^2,\ A_2 = b^2 l_1 + \omega^2 l_4, \tag{2.2}$$

$$G = \frac{1}{l_1 l_7 + l_1 l_5 l_{10}}(A_1 l_7 + A_2 l_1 l_{10} + A_1 l_5 l_{10} - b^2 l_2 l_3 + b^2 l_1 l_6 - b^2 l_2^2 l_{10} + b^2 l_1 l_5 + b^2 l_3 l_5 l_8 + b^2 l_1 l_7 l_9 - b^2 l_2 l_7 l_8), \tag{2.3}$$

$$N = \frac{1}{-l_1 l_7 - l_1 l_5 l_{10}}(-A_1 b^2 l_6 - A_1 A_2 l_{10} + b^4 l_2^2 + b^4 l_2 l_3 l_9 - b^4 l_1 l_6 l_9 + b^4 l_2 l_6 l_8 - A_2 b^2 l_1 - A_2 b^2 l_3 l_8 - A_1 b^2 l_5 - A_1 b^2 l_7 l_9), \tag{2.4}$$

$$F = \frac{1}{l_1 l_7 + l_1 l_5 l_{10}}(A_1 A_2 b^2 + A_1 b^4 l_6 l_9), \tag{2.5}$$

$$L_{1i} = \frac{-l_1 l_7 r_i^4 + l_1 l_6 b^2 r_i^2 + A_1 l_7 r_i^2 - b^2 l_2 l_3 r_i^2 - A_1 b^2 l_6}{-ibl_2 l_7 r_i^3 + ibl_3 l_5 r_i^3 - ibl_3 A_2 r_i + ib^3 l_2 l_6 r_i}, \tag{2.6}$$

$$L_{1(i+3)} = \frac{-l_1 l_7 r_i^4 + l_1 l_6 b^2 r_i^2 + A_1 l_7 r_i^2 - b^2 l_2 l_3 r_i^2 - A_1 b^2 l_6}{ibl_2 l_7 r_i^3 - ibl_3 l_5 r_i^3 + ibl_3 A_2 r_i - ib^3 l_2 l_6 r_i}, \tag{2.7}$$

$$L_{2i} = \frac{l_1 r_i^2 - A_1 - ibl_2 r_i L_{1i}}{ibl_3 r_i},\ L_{2(i+3)} = \frac{l_1 r_i^2 - A_1 + ibl_2 r_i L_{1(i+3)}}{-ibl_3 r_i}, \tag{2.8}$$

$$L_{3i} = ib - l_{11} r_i L_{1i} - l_{12} r_i L_{2i},\ L_{3(i+3)} = ib + l_{11} r_i L_{1(i+3)} + l_{12} r_i L_{2(i+3)},\ L_{4i} = ibl_{11} - l_5 r_i L_{1i} - l_7 r_i L_{2i}, \tag{2.9}$$

$$L_{4(i+3)} = ibl_{11} - l_5 r_i L_{1(i+3)} - l_7 r_i L_{2(i+3)},\ L_{5i} = -l_1 r_i + ibl_1 L_{1i} + ibl_6 L_{2i},\ L_{5(i+3)} = l_1 r_i + +ibl_1 L_{1(i+3)} + ibl_6 L_{2(i+3)}, \tag{2.10}$$

$$L_{6i} = -r_i l_9 + ibl_9 L_{1i} - ibL_{2i},\ L_{6(i+3)} = r_i l_9 + ibl_9 L_{1(i+3)} - ibL_{2(i+3)},\ L_{7i} = ibl_{13} - r_i L_{1i} + l_{10} r_i L_{2i},\ L_{7(n+3)} = ibl_{13} + r_n L_{1(n+3)} - l_{10} r_n L_{2(n+3)}. \tag{2.11}$$

ORCID iD

Mohamed I.A. Othman https://orcid.org/0000-0002-9577-5479
Ebtesam E.M. Eraki https://orcid.org/0000-0003-2234-3648
Mohamed F. Ismail https://orcid.org/0000-0001-8537-2222

How to cite this article: Othman M.I.A., Eraki E.E.M., Ismail M.F. Mathematical Model of a Thermoelastic Micro-elongated Plate Influenced by Initial Stress and an Upper Load from a Piezoelectric Layer according to Dual-phase-lag Model, *J. Appl. Comput. Mech.*, 11(3), 2025, 787-796. https://doi.org/10.22055/jacm.2024.47890.4818